

Design Considerations for Large Detector Arrays on Submillimeter-wave Telescopes

Antony A. Stark

Smithsonian Astrophysical Observatory, 60 Garden St. MS78, Cambridge, MA 02138, USA

ABSTRACT

The emerging technology of large ($\sim 10,000$ pixel) submillimeter-wave bolometer arrays presents a novel optical design problem—how can such arrays be fed by diffraction-limited telescope optics where the primary mirror is less than 100,000 wavelengths in diameter? Standard Cassegrain designs for radiotelescope optics exhibit focal surface curvature so large that detectors cannot be placed more than 25 beam diameters from the central ray. The problem is worse for Ritchey-Chretien designs, because these minimize coma while increasing field curvature. Classical aberrations, including coma, are usually dominated by diffraction in submillimeter-wave single dish telescopes. The telescope designer must consider (1) diffraction, (2) aberration, (3) curvature of field, (4) cross-polarization, (5) internal reflections, (6) the effect of blockages, (7) means of beam chopping on- and off-source, (8) gravitational and thermal deformations of the primary mirror, (9) the physical mounting of large detector packages, and (10) the effect of gravity and (11) vibration on those detectors. Simultaneous optimization of these considerations in the case of large detector arrays leads to telescopes that differ considerably from standard radiotelescope designs. Offset optics provide flexibility for mounting detectors, while eliminating blockage and internal reflections. Aberrations and cross-polarization can be the same as on-axis designs having the same diameter and focal length. Trade-offs include the complication of primary mirror homology and an increase in overall cost. A dramatic increase in usable field of view can be achieved using shaped optics. Solutions having one to six mirrors will be discussed, including a possible six-mirror design for the proposed South Pole 10m telescope.

Keywords: submillimeter, aberrations, field-of-view, detector arrays

1. INTRODUCTION

It will be possible in the coming decade to construct arrays of submillimeter-wave detectors having 10^3 to 10^4 pixel elements.¹ This is an exciting prospect because there is important science to be done at these wavelengths, observational work that requires deep imaging capability over large areas of sky. There is, however, a problem: an array of $N \times N$ pixels requires a telescope whose field of view is larger than N beams in diameter, and no such submillimeter-wave telescope exists for $N \gtrsim 25$. Design of such a telescope is a novel optical problem which differs significantly from the optical design problems encountered for visual wavelength telescopes, essentially because submillimeter-wave telescope apertures are only $\sim 10^5$ wavelengths across.

The problem can be summarized thus:

1. An aperture $D \sim 10$ m is needed to provide the sensitivity and resolution to meet science goals.
2. If a detector array has 100×100 pixels, the telescope field of view must be at least $\sqrt{2} \cdot 100 \cdot \lambda/D \sim 0.8^\circ$ in diameter.
3. Visual wavelength telescopes 10 m in diameter don't have well corrected fields of view which are 0.8° in diameter because of optical aberrations. Visual wavelength telescopes can feed very large CCD arrays, but only because they have $D/\lambda > 10^6$. Many pixels then fit within a field of view that is $\sim 0.3^\circ$ in diameter.
4. Radio and submillimeter telescopes 10 m in diameter with fields of view 0.8° in diameter have large and mechanically awkward secondary and ancillary optics.

This paper discusses aspects of this problem and offers some design solutions. In §2, the science goals are discussed, to indicate the type of observation needed. In §3, submillimeter telescope designs are compared in sensitivity and resolution, to show that design and construction of a wide field submillimeter telescope is desirable. The design of wide-field submillimeter telescopes having one or more optical elements is treated in §4.

Other author information: E-mail: aas@cfa.harvard.edu; WWW: <http://cfa-www.harvard.edu/~aas/tenmeter>

2. SUBMM SCIENCE WITH LARGE DETECTOR ARRAYS

Primary cosmic microwave background anisotropy at arcminute scales. Current CMBR observations² show a clear maximum in the anisotropy spectrum at a spatial scale near 1° . The damping tail region at arcminute scales provides a test of the acoustic oscillation model. The shape of the damping tail is a manifestation of the speed at which the recombination process occurs, and the degree to which recombination is mixed with re-ionization. To study primary anisotropy at arcminute angular scales, it will be important to simultaneously understand the secondary contribution to anisotropy due to Sunyaev-Zel'dovich (S-Z) distortion in galaxy clusters between the recombination last scattering surface and the observer. The 200-300 GHz range of frequencies are needed to allow spectral separation of thermal S-Z effect from primary anisotropy. Since there are 10^4 to 10^5 visible clusters of galaxies, a small beam size is needed at 200-300 GHz to locate the cluster-free regions of sky that will be observed for primary anisotropy studies (see Figure 1).

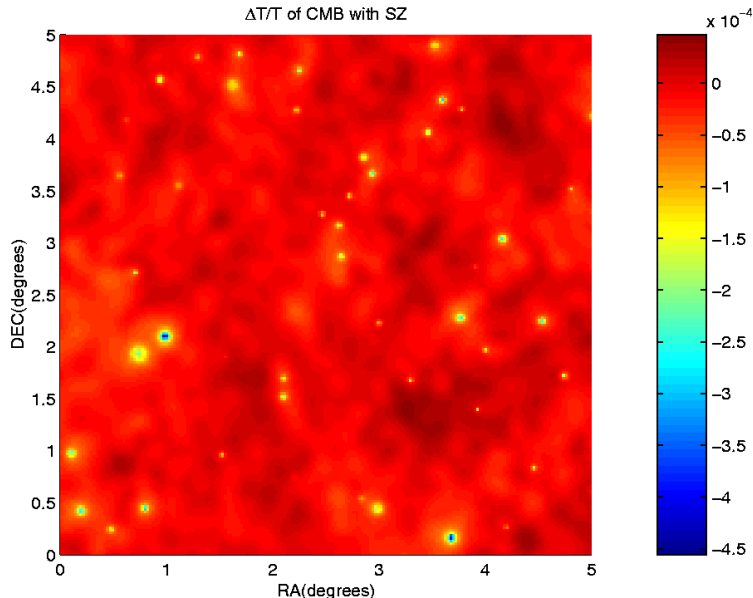


Figure 1. Simulated Fine Angular Scale CMBR Image³. Simulated CMBR structure on a twenty-five square degree region of sky. The faint extended structure is primary CMBR anisotropy, while the strong localized sources are secondary anisotropy due to the Sunyaev-Zel'dovich effect in galaxy clusters. In this model, S-Z signal dominates at fine angular scales. The simulation does not include the S-Z filaments expected from the collapse of 100 Mpc structures.

Sunyaev-Zel'dovich effect in known clusters. As CMBR photons travel from the surface of last scattering to the observer, secondary anisotropies can arise due to the interaction of the CMBR photons with intervening matter. Of particular interest is the S-Z effect, which occurs when CMBR photons travel through a cluster of galaxies.⁴ Approximately 10% of the total mass of rich clusters of galaxies is in the form of hot ($\sim 10^8$ K) ionized plasma. Compton scattering of CMBR photons by electrons in this intra-cluster plasma can result in an optical depth as high as 0.02, resulting in a distortion of the CMBR spectrum at the mK level.

The thermal component of the S-Z effect can be used in combination with X-ray data to provide a measure of the Hubble constant (H_0). In addition, when combined with a measurement of electron temperature, the ratio of the kinematic and thermal component amplitudes provides a direct measurement of the cluster's peculiar velocity relative to the rest frame of the CMBR. The observed surface brightness difference of both the thermal and kinematic components is independent of the cluster redshift, as long as the cluster is resolved. Clusters are large objects, typically of order 1 Mpc, and subtend an arcminute or more at any redshift, so all clusters will be resolved with a

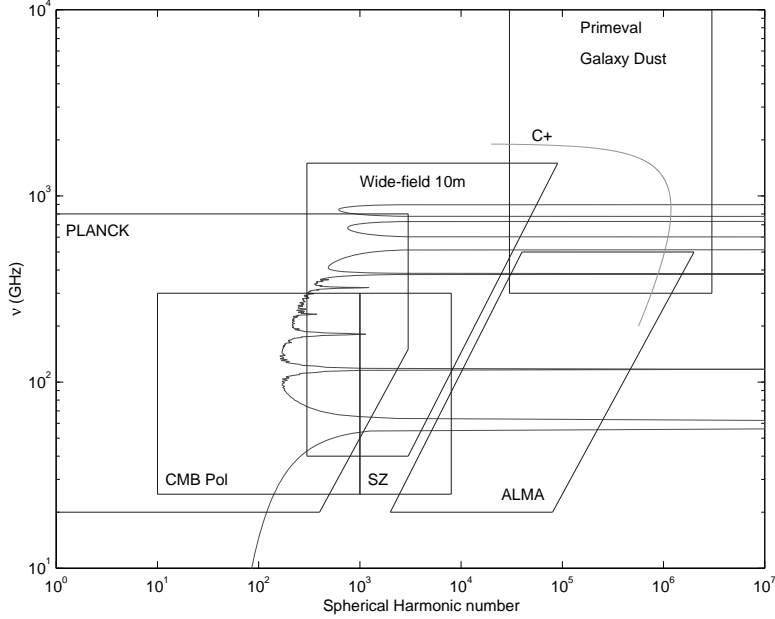


Figure 2. A Comparison of Telescopes for CMBR³. Shown in angular scale l vs. observing frequency ν are science targets: CMBR polarization, Sunyaev-Zel’dovich effect, dust emission by primeval galaxies, and the fine structure line of ionized carbon from galaxies. Also shown are the domains of three instruments: the Planck spacecraft, a wide-field 10m, and the Atacama Large Millimeter Array (ALMA). The jagged curve is a comparison of atmospheric noise to noise in a spacecraft environment. On this curve, the South Pole winter atmospheric emission fluctuations equal the photon fluctuations in a spacecraft environment (assumed to be caused by the brightness of the sky plus photons emitted from a 1% emissivity 70 K surface). Observations above and to the left of this curve derive a noise benefit from being in space. Cluster S-Z observations fall to the right of the noise boundary, and are best done with a wide-field 10m. The NASA Cosmic Microwave Background Future Missions Working Group³ recommends that most CMBR polarization observations be done from space, but high spatial frequency CMBR polarization can also be measured with the 10m telescope.

10m telescope. Accurate S-Z measurements can be made throughout the Universe, all the way back to the epoch of formation of the hot intra-cluster gas.

Sunyaev-Zel’dovich effect blank-sky survey. The fast survey capability of a wide-field submillimeter telescope will allow detection of S-Z effect in blank-sky searches. Detections of small-scale decrements in CMBR intensity not associated with known clusters may have been discovered by Ryle Telescope⁵ and VLA⁶ observations. These may be due to the S-Z effect in very distant clusters. As shown in Figure 1, serendipitous detection of distant clusters will necessarily occur in studies of arcminute-scale CMBR primary anisotropy. These detections, both with and without additional X-ray data,⁷ allow powerful tests of cosmological models and galaxy formation theories. In particular, the cluster counts are sensitive to Ω_Λ and provide an independent check of type Ia supernova results.

S-Z effect also results from low density, warm baryonic gas between clusters.⁸ Models of structure formation predict that most of the baryonic matter in the Universe is located in intra-cluster filaments which are responsible for the Ly- α forest seen in quasar spectra. The S-Z effect caused by the filaments can be directly imaged, permitting study of the filaments in the spaces between quasars.

Continuum detection of high redshift protogalaxies not detectable in the visible or near-IR. Most of the luminosity resulting from the collapse energy of galaxies and the first generations of stars may not appear at visual or near-infrared wavelengths (even in the rest frame of the distant galaxy), but may instead be reradiated by dust.^{9,10} Detection of the cosmic far-infrared background radiation¹¹ (CFIRBR) is evidence that most of the energy released in the initial collapse of galaxies and the creation of metals appears at the current epoch as submillimeter-wave radiation. In a recent review of work on the Hubble Deep Field (HDF), P. Madau wrote that “the poorly constrained amount of starlight that was absorbed by dust and reradiated in the far-IR at early epochs represents one of the biggest uncertainties in our understanding of the evolution of luminous matter in the universe”.¹²

Within the next decade, submillimeter studies of known sources at high redshift will be carried out with powerful interferometer arrays, the SMA and the ALMA, at least at longer submillimeter wavelengths. A fundamental contribution of wide-field single dish submm telescopes will be to detect and locate high redshift sources by studying the structure of the CFIRBR on a scale of $\sim 10''$. Such work has already begun on Mauna Kea. At $850\mu\text{m}$ wavelength, SCUBA^{13,14} has observed a 10 square arcminute field to an rms noise level of 2 mJy beam^{-1} and a 6 square arcminute field centered on the HDF to an rms noise level of 0.5 mJy beam^{-1} . These surveys show detected source number densities of about 1 per square arcminute, where at least some sources are at $z \sim 0.3$ to 4 and have inconspicuous (or possibly no) optical counterparts.^{15,16} Some models of protogalaxies consistent with a protogalactic origin for the CFIRBR¹⁷ predict hundreds of sources per square degree which are detectable at the $\geq 1\text{ mJy}$ level in the submillimeter, but which have optical counterparts below the detection limit of the HST HDF image.

3. TELESCOPE SENSITIVITY

Table 1. Continuum Sensitivity of Submillimeter Telescopes

Telescope	A^a (m^2)	R^b ($''$)	S^c	NEFD ^d			Time in hours to survey		
				(mJy s ^{1/2})			1 square degree at 1 mJy		
				850 μm	450 μm	350 μm	850 μm	450 μm	350 μm
wide-field 10 m	79	11	200	<i>60</i>	<i>64</i>	<i>74</i>	<i>18</i>	<i>20</i>	<i>27</i>
wide-field 30 m	711	4	22	<i>7</i>	<i>7</i>	<i>8</i>	<i>2</i>	<i>2</i>	<i>3</i>
AST/RO	2	65	92	<i>2160</i>	<i>2300</i>	<i>2660</i>	5.1×10^4	5.8×10^4	7.7×10^4
JCMT	177	7	5	80	700	760	1.3×10^3	9.8×10^4	1.2×10^5
CSO	79	11	11	<i>150</i>	2000	2200	2.0×10^3	3.6×10^5	4.4×10^5
SOFIA	5	44	50		<i>200</i>	<i>200</i>		800	800
FIRST	7	32	4.3		<i>54</i>	<i>54</i>		678	583
“submm CBI” ^e	8.3	11	4	<i>297</i>	<i>2529</i>	<i>2768</i>	6.2×10^3	1.6×10^6	1.1×10^7
SMA	227	2	0.14	<i>134</i>	<i>1142</i>	<i>1250</i>	3.6×10^4	9.3×10^6	1.9×10^7
MK array ^f	483	0.5	0.02	<i>59</i>	<i>719</i>	<i>790</i>	4.9×10^4	2.6×10^7	5.2×10^7
MMA	2010	0.2	0.08	<i>7</i>	<i>45</i>	<i>52</i>	<i>230</i>	3.4×10^4	7.5×10^4
ALMA	7000	0.2	0.06	<i>2</i>	<i>12</i>	<i>15</i>	<i>19</i>	2.4×10^3	6.4×10^3

Notes:

a. Telescope area (m^2)

b. Resolution element (arcsec) for $\lambda = 450\mu\text{m}$. Resolution element scales as λ .

c. Instantaneous sky coverage (arcmin^2) for $\lambda = 450\mu\text{m}$. Instantaneous Sky Coverage scales as λ^2 for interferometers, is independent of λ for most single-dish instruments, and is 4.3, 5.0 and 2.7 arcmin^2 at $480\mu\text{m}$, $350\mu\text{m}$ and $250\mu\text{m}$, respectively, for FIRST (G. Pilbratt, personal communication).

d. Noise Equivalent Flux Density, the sensitivity to point sources whose positions are known. Numbers in italics are predicted sensitivities; numbers not in italics are measured, on-the-telescope values and are subject to downward revision with improved techniques. Predicted sensitivities are optimistic in the sense that in all cases they are near the thermal background limit, a limit that has not yet been achieved in practical submillimeter-wave bolometer systems. This table is based on the work of Hughes and Dunlop.¹⁸

e. A hypothetical submillimeter-wave array with the configuration of the CBI; the actual CBI operates at $\lambda \sim 1\text{ cm}$.

f. Mauna Kea array consisting of the SMA, the CSO, and the JCMT

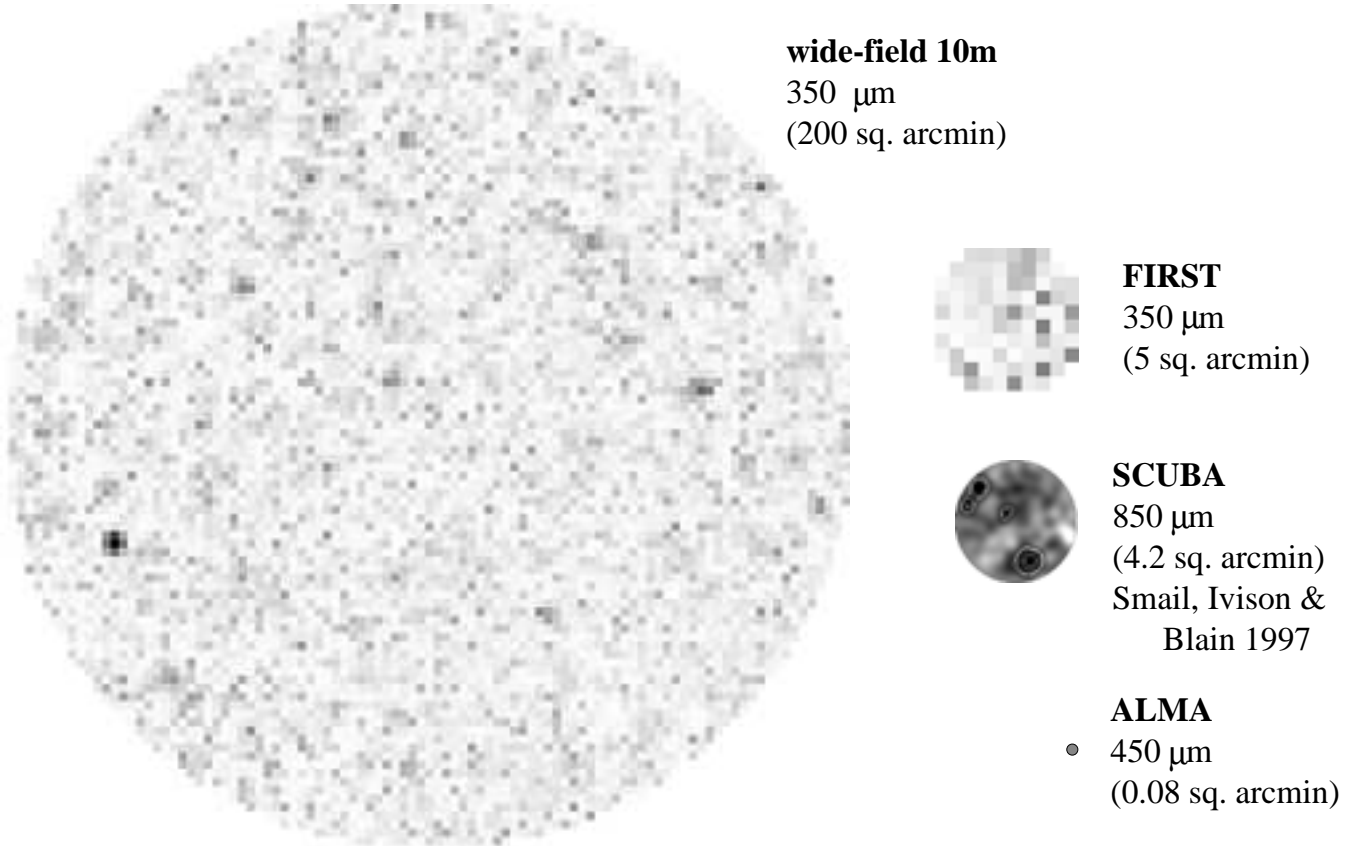


Figure 3. Image Sizes of Submillimeter-wave Telescopes. Simulated images from a wide-field single dish 10m and FIRST are compared to SCUBA results¹³ and the image size of the ALMA. The simulated data for the single dish and FIRST are the Guiderdoni et al. protogalaxy Scenario B model¹⁷ observed to an rms noise level of 1 mJy per pixel with a broad-band bolometer array. This noise level is attainable with about two hours of on-source time at the wide field single dish and 20 minutes of on-source time with FIRST. It is assumed that the protogalaxies are Gaussian distributed (i.e., not clustered). A black pixel corresponds to 78 mJy, a white pixel is 0 mJy, and the greyscale is linear. The single dish plot shows over 500 individual sources at the 5σ level.

Table 1 shows the continuum sensitivity and beam size of submillimeter-wave telescopes and illustrates the strength of wide field single dish for deep continuum surveys. The NEFD values in this table for each of the instruments originate if possible from the scientific group operating or proposing that instrument; they are a mixed bag of actual results on the telescope and calculations, some of which are based on optimistic assumptions. A surprising implication of Table 1 is that a wide field single dish is faster at submillimeter detection of protogalaxies than the ALMA and FIRST. Is this plausible, given that these instruments are at least an order of magnitude more expensive? Suppose we are conducting a large-scale survey at $\lambda 450\mu\text{m}$ for point-source objects at an rms flux density F_{limit} . The time required for 1σ detection in one pixel of a map of the sky is given by the radiometer equation

$$t_{limit} = \frac{(2kT_{sys})^2}{B(\eta AF_{limit})^2} = \left(\frac{\text{NEFD}}{F_{limit}} \right)^2, \quad (1)$$

where

$$T_{sys} = (T_{receiver} + \eta T_{atmosphere}[1 - e^{-\tau}] + [1 - \eta]T_{ambient}) \frac{e^{\tau}}{\eta}$$

is the atmosphere-corrected effective system temperature, A is the total collecting area of the telescope, η is telescope

Table 2. Bolometer Array Instruments

Instrument	Current Status	Number of Detectors, n	Web Reference
SCUBA	operational	128	http://www.jach.hawaii.edu/JACpublic/JCMT/scuba
BOLOCAM	in development	151	http://binizaa.inaoep.mx/pub/ins/pres_cam
SAFIRE	in development	2,048	http://pioneer.gsfc.nasa.gov/public/safire
SPECS	proposed	60,000	http://www.gsfc.nasa.gov/astro/specs

efficiency, τ is the atmospheric opacity at the elevation angle of the observation, and B is the pre-detection bandwidth. $T_{atmosphere} \approx T_{ambient} \approx 200$ K at the South Pole and ≈ 260 K at mid-latitude sites. Here we neglect polarization, relative sideband gain, the distinction between telescope efficiency and aperture efficiency, digitization and data processing corrections: these introduce factors of order unity which have been considered in Table 1 but which can be neglected in the present plausibility argument. We assume that the radiometer is switched rapidly enough to filter out sky noise. Equation 1 is then approximately correct regardless of whether the system is heterodyne or bolometric, or whether the collecting area, A , is arranged in multiple antennas or a single dish. All telescopes will be designed for reasonably high efficiency, $\eta \sim 0.9$. Future submillimeter-wave systems will be background-limited, meaning that the $T_{receiver}$ term will be smaller than the atmospheric ($T_{atmosphere}$) and telescope background ($T_{ambient}$) terms. When $\tau > 1$, as it often is for ground-based submillimeter-wave observations, the opacity-correction term, e^τ , dominates all other effects: $T_{sys} \approx e^\tau (T_{atmosphere} + T_{receiver}/\eta)$, and $t_{limit} \propto \exp(2\tau)$; in this case relatively small improvements in τ make a large difference. At $\lambda 450\mu\text{m}$ and 45° elevation the 25% opacity values in winter are $\tau \lesssim 0.36$ at the South Pole and $\tau \lesssim 0.79$ at Chajnantor. When τ is small or zero, for example in space or on the ground at centimeter wavelengths, then the telescope background $(1 - \eta)T_{ambient}$ dominates. For a single dish located at the South Pole, $T_{sys} \simeq 1000$ K (a value that is often surpassed on AST/RO), for the ALMA, $T_{sys} \simeq 2500$ K (this high system temperature is due mostly to atmospheric opacity), and for FIRST, $T_{sys} \simeq 50$ K (the low background of a cooled telescope in space). For the wide-field single dish $B \simeq 100$ GHz, for FIRST, $B \simeq 200$ GHz, whereas for the ALMA $B \simeq 16$ GHz. We therefore conclude that the time required to achieve a $F_{limit} = 1\text{mJy}$ noise level, t_{mJy} , is about four hours for the wide-field single dish, forty minutes for FIRST, and one minute for the ALMA. To reach an rms noise of, say, 0.1 mJy would require 100 times longer integration in each case. ALMA and FIRST are both faster than the ground-based single dish at detecting individual sources.

Now we note that the area of sky covered by the field of view during this integration time, the “instantaneous sky coverage” (S in Table 1, see Figure 3), is very different for the three telescopes. For the wide field 10m, S is over an order-of-magnitude larger than FIRST and nearly four orders-of-magnitude larger than the ALMA (see Figure 3). An efficient configuration of n diffraction-limited detectors (bolometer pixels or heterodyne receivers) on a telescope of total area A will yield an instantaneous sky coverage of $S \approx \frac{n\lambda^2}{\eta A}$. The speed at which the the sky can be mapped is S/t_{limit} . A figure of merit for blank sky surveys can therefore be defined:

$$\text{survey speed} \propto \text{figure of merit} \equiv \frac{nB\eta A}{T_{sys}^2}. \quad (2)$$

The trade-offs in survey speed between a wide-field single-dish telescope and an array instrument like the ALMA can be estimated by evaluating Equation 2. Suppose the single dish telescope has a focal plane array containing $N \times N$ detectors, and the interferometer consists of E antenna elements, each with the same diameter as the single-dish telescope, and each having one heterodyne receiver. Then $S_{dish} = N^2 S_{interferometer}$, $A_{interferometer} = EA_{dish}$, $n_{interferometer} = E$, and $n_{dish} = N^2$. If the two instruments have the same T_{sys} , the single dish telescope will be faster in survey mode by a factor

$$\frac{N^2}{E^2} \frac{B_{dish}}{B_{interferometer}}.$$

Comparing the wide-field 10m with the ALMA, $N \simeq 100$, $E \simeq 80$, and $B_{\text{dish}}/B_{\text{interferometer}} \simeq 8$. *The single-dish 10m is at least an order-of-magnitude faster than the ALMA at submillimeter-wave sky surveys.* It might be argued that N^2 detectors represents a lot of complex electronics, and that for large numbers it may be easier to build E whole antennas than N^2 detectors—however, any interferometer will necessarily have E^2 correlators; these correlators are likely to be more complex than the photolithographically-produced detector plus amplifier plus multiplex needed for each of the N^2 pixels of a bolometer array. Table 2 shows the number of detectors, n , in some current and proposed millimeter and submillimeter instruments. The large jump in n between the current version of BOLOCAM and SAFIRE reflects the development of cryogenic multiplex readouts. Compared to single-dish maps, maps made by the interferometric instrument have much higher resolution and positional accuracy, but the rate at which the maps are made is at least an order-of-magnitude slower and the initial capital cost is at least an order-of-magnitude higher. It is a waste of scarce resources to map large areas of blank sky with the ALMA. Note too that at a survey speed of $\sim 2.4 \times 10^3$ hours per square degree, the ALMA will not be able to survey more than a hundred square degrees during its operating lifetime, but there are many thousands of square degrees containing potentially interesting sources. The best strategy to detect and study protogalaxies is to survey the sky quickly with the relatively inexpensive single dish and then study the detected sources in detail with the ALMA.

For speed and coverage in deep surveys, a wide-field telescope can pursue an optimization strategy:

1. Build a reflector whose beamsize is equal to the spatial scale of interest.
2. Make the telescope losses, blockage and spillover as small as possible at the frequencies of interest.
3. Make the field of view as large as possible.
4. Populate that field of view with as many broadband detectors as possible.
5. Place the telescope at the best possible site.

Such a wide-field single dish is an “optimal design” for the discovery of objects at spatial frequencies near $\frac{1}{2}D/\lambda$.

4. TELESCOPE DESIGN

The physical size of a single pixel in an array of bolometer detectors must be half a wavelength or more in order to efficiently couple power into the detector. If the pixel size is as small as a wavelength, the beam impinging on the bolometer array must be highly convergent (have an $f/d \equiv F_{\text{detector}} \lesssim 1$), since the beamwaist diameter¹⁹ at the detector is $\approx \lambda F_{\text{detector}}/\pi$. A submillimeter-wave detector array containing N^2 pixels will necessarily be $N F_{\text{detector}}/\pi$ wavelengths across, or about 3 cm for a 100×100 array. Suppose the telescope which will feed the array has an aperture D and an effective focal length f_e . Then a diffraction-limited beam on the sky will have an angular width of λ/D . The telescope field of view must be about $2N$ beams across to fully feed the array and allow for beam chopping. Let the desired field of view be $\zeta N \lambda/D$ where $\zeta \sim 1.5$ is an arbitrary parameter to allow for illumination of the corners of the array and the extra field of view needed for chopping. At the surface of the detector, this field of view has a physical size $\zeta N \lambda f_e/D = \zeta N \lambda F_e$. The telescope must provide a field of view at least this large such that aberrations are small compared to the pixel size.

4.1. Prime focus

A prime focus feed is the simplest possible design. The detector array is designed for a focal ratio F_{detector} , so perhaps it can be matched by simply placing it at the focus of a single reflector having a focal ratio $F \equiv f/D = F_{\text{detector}}$. This will, in fact, match the central pixel and provide the correct plate scale (overall magnification of the telescope in, e.g., millimeters per arcsecond) to match the immediately surrounding pixels to adjacent beams on the sky.

A field of view the size of the array must have sufficiently small aberrations. The dominant aberrations for a single paraboloidal reflector are coma and astigmatism. The angular coma is $\theta_c = \frac{\theta}{16F^2}$, and the angular astigmatism is $\theta_a = \frac{\theta^2}{2F}$, where θ_c and θ_a are the angular blur due to coma and astigmatism for a beam at angle θ from the center of the field.²⁰ The angular blur due to diffraction is $\theta_d = \lambda/D$, so the coma blur is less than the diffraction blur

for field angles $\theta \lesssim 16F^2\lambda/D$, and the astigmatic blur is less than the diffraction blur for field angles $\theta \lesssim \sqrt{2F\lambda/D}$. These aberrations place two constraints on the mirror optics:

$$F \gtrsim \sqrt{\frac{\zeta N}{32}}, \quad (3)$$

and

$$f = FD \gtrsim \frac{1}{2} \zeta^2 N^2 \lambda. \quad (4)$$

For a submillimeter-wave telescope operating with a large detector array, Equation 3 requires that $F \gtrsim 2.2$, while Equation 4 requires that $f \gtrsim 10\text{m}$. A reflector satisfying these constraints will have an acceptable image, but it makes for a telescope design with five disadvantages:

1. The F number is much bigger than the values usually chosen for radiotelescopes, resulting in a large, elongated structure. Most radiotelescopes have $F \sim 0.5$ for the primary mirror.
2. Since there is no chopper mirror, there is no way to rapidly switch the position of the array on the sky—the entire telescope must be moved.
3. The detector package must tilt with the movement of the telescope. If the telescope system is ground-based, the direction of gravity will rotate by 90° with respect to the detector and its cryogenics system as the telescope moves in elevation.
4. The detector package blocks the primary mirror.
5. Since $F_{\text{detector}} = F > 2.2$, the size of the detector package and the size of the opening into the cryogenics will be larger than optimal.

Problem 4, the blockage of the primary, can be avoided by using an off-axis section of the parabola. This brings with it additional problems of cross-polarization and asymmetric illumination, but for a system with large F number these will not be large effects. An off-axis single reflector has about the same aberrations as an on-axis reflector with the same focal length and twice the aperture, so the F number of the off-axis system must be about twice as large as the value given by Equation 3.

Problems 2 and 3 could be obviated by placing the telescope in space. Imagine a spacecraft with a large submillimeter detector package fed by a ~ 2 m diameter off-axis mirror with a ~ 10 m focal length. This instrument would scan in a “stare” mode and would produce maps with a resolution about $1'$.

A possible variant of the single mirror offset telescope is a primary mirror with a flat or nearly flat secondary. This mirror could fold the beam back below the primary mirror and act as a chopper—a kind of folded Newtonian. Such a mirror might also act as an aspheric corrector, providing a better compromise between spherical aberration and coma, or providing correction for a spherical primary.

4.2. Cassegrain and Gregorian designs

The addition of a second curved mirror brings considerable additional freedom and improved performance to telescope design. Cassegrain designs, with a concave primary and a convex secondary, are ubiquitously successful from visual to radio wavelengths. The reasons for this success differ at different wavelengths. At radio wavelengths, the design criterion is to provide high aperture efficiency and minimal blockage for a single beam or a few beams near the center of the field of view. At visual wavelengths, the design criterion is to provide a field of view about $10'$ across which is free of coma, the otherwise dominant aberration—this is accomplished by the aplanatic Cassegrain (or Ritchey-Chretien) which reduces coma to less than a second of arc at the expense of increased image curvature. The submm telescope problem is novel because a large field of view is needed in a situation where diffraction dominates the classical aberrations, and it is curvature of field rather than coma which tends to limit the field of view. These issues were discussed at an earlier SPIE conference.²¹

A telescope having only two mirrors would not be used to feed a submillimeter-wave detector array directly. Large submillimeter-wave detector arrays require a small value for F_{detector} ($\lesssim 3$) so that the detector size is manageable,

whereas two mirror telescopes have large values of F_e ($\approx 1.5 \cdot (\text{focal length of primary})/(\text{diameter of secondary}) \sim 30$). At least a few additional optical elements are needed as focal reducers. If the primary and secondary produce a sufficiently corrected image with a suitably large field of view, additional optics can feed that image onto the array.

Let R_1 and R_2 be radius of curvature at the vertex of the primary and secondary mirrors, respectively. The focal length of the primary mirror is half the radius of curvature, $f_1 = R_1/2$. Let $m \equiv 2f_e/R_1$ be the magnification of the secondary. If the secondary is made as small as it can be without vignetting the center of the field, then the ratio of the diameter of the secondary, D_2 , to the diameter of the primary, D_1 , is $k \equiv \frac{D_2}{D_1} = \frac{R_2}{R_1} \frac{m-1}{m}$. The distance from the back of the primary to the focus of the two-mirror system is $f_1\beta \equiv f_1[k(m+1) - 1]$, where β is the “scaleless backfocal distance” and is either positive or negative depending on whether the focus is behind or before the primary mirror. These variables and their sign conventions are as defined by Schroeder.²⁰

Consider first a conventional on-axis design. The beam passes through a hole in the primary mirror, and the hole in the primary should be no larger than D_2 , the diameter of the secondary. The diameter of the image is

$$D_i \equiv \zeta N \frac{\lambda}{D_1} f_e = \zeta N \lambda m F_1. \quad (5)$$

To avoid vignetting, D_i must be smaller than or equal to the diameter of the central hole in the primary, which must be smaller than or equal to the diameter of the secondary, D_2 . But as D_2 becomes smaller, $|m|$ becomes larger and D_i becomes larger. The best that can be done is to make D_2 , D_i , and the hole in the primary the same size. Letting $D_2 = D_i$ in Equation 5 and substituting for k and m yields a quadratic equation that can be solved for D_2 :

$$D_2 \geq D_i = \frac{1}{2} \zeta N \lambda F_1 \left[\sqrt{\frac{4(1+\beta)D_1}{\zeta N \lambda F_1} + 1} - 1 \right] \approx \sqrt{(1+\beta)\zeta N \lambda f_1}. \quad (6)$$

This is a minimum size for the secondary mirror of a two mirror telescope to feed an $N \times N$ array at wavelength λ . For a 10m diameter $F_1 = 0.4$ telescope feeding an $N = 100$ array at $\lambda = 1\text{mm}$, $D_2 \gtrsim 1.1\text{m}$. This is considerably larger than the secondary mirrors usually fitted to Cassegrain systems. In order to feed a 100×100 array, the CSO and JCMT would have to be refitted with secondary mirrors (and primary mirror openings) which are about twice as large as the current ones. Antennas designed as elements of interferometric arrays are particularly bad, since they are highly optimized to feed a single beam with high efficiency and therefore have minimal secondaries.

Ancillary optics. If the value of D_2 satisfies Equation 6, it is possible to achieve a $\approx 1^\circ$ diameter field of view at $\lambda = 1\text{mm}$ with a $D_1 = 10\text{m}$ Cassegrain or Gregorian. The dominant aberration is curvature of field; such a telescope has a surface of best images which resembles a 3 steradian cap on a 1.5 m diameter sphere (concave toward the secondary in a Cassegrain and convex toward the secondary in a Gregorian).

Additional optics are needed to match a Cassegrain or Gregorian focus to a detector array, and these can be used to correct some of the deficiencies in the quality of focus. In particular a field-flattening mirror is a mirror placed at the telescope focus which has the same direction of curvature as the focal plane. The surfaces of best images will be flattened when the beam is refocused by subsequent optics,

The ancillary optics in a wide field telescope of conventional telescope design will be large—one to three meters in diameter, in order to handle an image as large as that given by Equation 6, and the further behind the primary backup structure they are located, the larger they must be (since D_i increases with increasing β). This creates problems in structural design. Large cavities with big mirrors need to be located within the support structure of primary mirror. If the telescope has a Nasmyth focus, the hole in the elevation bearing must be large.

Offset optics. An off-axis design for the primary mirror helps solve this problem. If the receiver does not block the primary, then β can be negative, placing the focus of the secondary in front of but below the primary. This reduces the overall focal length, f_e and thereby reduces the size of the image. The ancillary optics are then both smaller and removed from the region behind the primary mirror. Figure 4 shows an off-axis Gregorian design that provides for beam chopping and has a 1° usable field of view. This design is very nearly a 1/10 model of the Green Bank Telescope,²³ because it solves similar design problems at approximately 1/10 the wavelength.

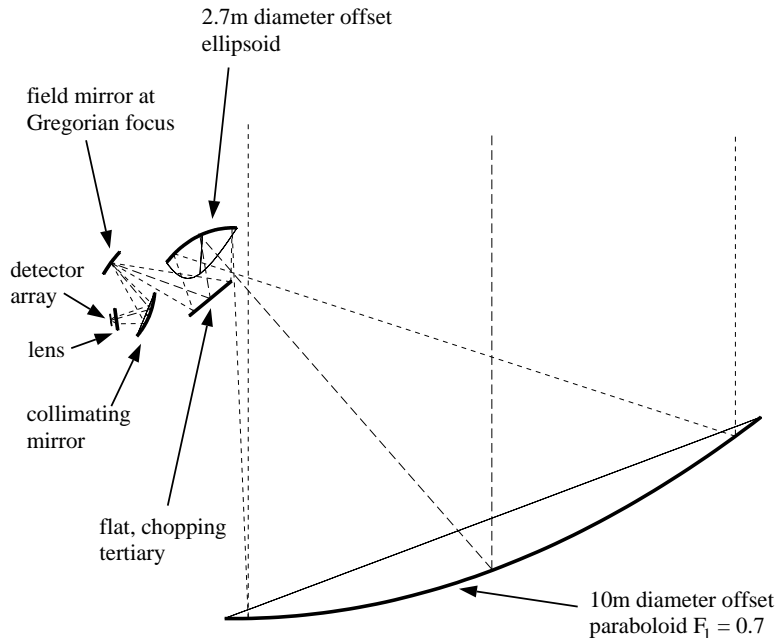


Figure 4. Scale drawing of a wide-field submm telescope. This is an offset Gregorian design with ancillary optics which provide beam chopping and a focal reducer to feed a large detector array. All optical elements are symmetric about the plane of the page; in a practical system the fourth and fifth mirrors would fold the beam so that it was parallel with the telescope’s elevation axis at the point where the beam entered the cryogenic dewar—this would allow the dewar to rotate around the beam and not tilt with telescope elevation. The primary and secondary are a conventional offset Gregorian design having $D_1 = 10\text{ m}$, $F_1 = 0.7$ and $\beta = -0.7$, except that the secondary is tilted to satisfy the Dragone²² relation with $i_0 = 0$. The flat tertiary is at an image of the aperture. The fourth and fifth mirrors are highly aspheric, offset, polynomial surfaces calculated to correct aberrations at the detector array. The fourth mirror is located at the Gregorian focus and acts as a field lens to image the exit pupil of the telescope onto the aperture stop of a focal reducer consisting of a collimating mirror and a lens. This telescope has a usable field of view about 1° at $\lambda = 1\text{ mm}$.

There is no optical penalty for using offset optics. Dragone²² has shown that if the offset angles in an offset two mirror telescope are chosen correctly, then aberrations and cross-polarization effects in that offset telescope are the same as those in a conventional on-axis antenna with the same diameter and focal length. The beam efficiency, aperture efficiency, and sidelobe levels in the off-axis antenna are better than those in the on-axis antenna, because in the on-axis design there will be diffraction, reflection, and blockage from the secondary mirror and its supports. An off-axis two mirror telescope with correctly chosen offset angles will always be optically superior to a similar on-axis configuration.

Avoidance of internal reflections is beneficial to the design of submillimeter-wave telescopes. Any receiver or detector placed at the focus of the instrument will necessarily emit into the telescope some amount of submillimeter-wave power in the band of interest. If there is a reflection in the system, for example at the secondary mirror some 6 meters distant, then a resonant cavity is formed whose modes are spaced at roughly 25 MHz intervals. Also critical to submillimeter-wave telescope design is minimization of variations in antenna thermal emissions as a function of chopper angle. Chopper offsets can more easily be minimized in an off-axis design. In an off-axis Gregorian the placement of the chopper at an image of the primary allows the beam to be steered on the sky without changing the illumination of the primary.

It is more expensive to build a telescope off-axis. Compared to an on-axis design of the same aperture, there are twice as many types of surface panels for the primary mirror. The primary backup structure is less symmetric,

making the structural design for homology more complex and increasing the number of dissimilar parts. These detriments are mitigated by the modern use of computers in design and manufacturing. A detailed consideration of the design problems for on-axis systems will likely show that for a given cost, an offset design can provide more pixels with a greater effective collecting area than an on-axis design.

5. CONCLUSION

The salient results of this investigation are:

1. There is important science to be done which requires large-scale imaging at submillimeter wavelengths.
2. Single-dish telescopes with large detector arrays are faster and more cost effective at mapping large areas of sky than are other telescope types. Such instruments are highly complementary to interferometric arrays, detecting sources to be studied in detail by interferometric techniques.
3. None of the existing designs for submillimeter-wave telescopes are capable of feeding large detector arrays. In particular, the secondary mirror must be large.
4. It is nevertheless possible to design a telescope which will accommodate large detector arrays while providing for beam chopping, if the design starts with a clean slate.

ACKNOWLEDGMENTS

I thank J. B. Peterson and C. Cantalupo of Carnegie-Mellon U. for Figures 1 and 2. This work was supported in part by the Smithsonian Institution and in part by the National Science Foundation under a cooperative agreement with the Center for Astrophysical Research in Antarctica (CARA), grant number NSF DPP 89-20223. CARA is a National Science Foundation Science and Technology Center.

REFERENCES

1. J. C. Mather, S. H. Moseley, Jr., D. Leisawitz, E. Dwek, P. Hacking, M. Harwit, L. G. Mundy, R. F. Mushotzky, D. Neufeld, D. Spergel, and E. L. Wright, "The submillimeter frontier: A space science imperative." *astro-ph/9812452*, 1998.
2. M. White, "CMB experiments." <http://cfa-www.harvard.edu/~mwhite/cmbexptlist.html>.
3. J. B. Peterson, J. B. Carlstrom, E. S. Cheng, M. Kamionkowski, A. E. Lange, M. Sieffert, D. N. Spergel, and A. Stebbins, "Cosmic Microwave Background observations in the post-Planck era," in *Report of the NASA Cosmic Microwave Background Future Missions Working Group*, 1999. <http://cmbr.phys.cmu.edu/future.html>.
4. M. Birkinshaw, "The Sunyaev-Zel'dovich effect," *Phys. Rept.* **310**, p. 97, 1999. *astro-ph/9808050*.
5. M. Jones, R. Saunders, J. Baker, G. Cotter, A. Edge, K. Grainge, T. Haynes, A. Lasenby, G. Pooley, and H. Rottgering, "Detection of a cosmic microwave background decrement toward the $z = 3.8$ quasar pair PC 1643+4631A,B," *ApJ* **479**, p. L1, 1997.
6. E. A. Richards, E. B. Fomalont, K. I. Kellermann, R. B. Partridge, and R. A. Windhorst, "Detection of a small scale cosmic background anisotropy," *AJ* **113**, p. 1475, 1997.
7. G. P. Holder and J. E. Carlstrom, "The Sunyaev-Zeldovich effect as microwave foreground and probe of cosmology," in *Microwave Foregrounds*, A. de Oliveira-Costa and M. Tegmark, eds., ASP, 1999.
8. R. Cen and J. P. Ostriker, "Where are the baryons?," *ApJ* **514**, p. 1, 1999.
9. G. R. Meurer, "The case for substantial dust extinction at $z \sim 3$," in *The Hubble Deep Field*, M. Livio, S. M. Fall, and P. Madau, eds., STScI Symposium Series, 1998. *astro-ph/9708163*.
10. C. Pearson and M. Rowan-Robinson, "Starburst galaxy contributions to extragalactic source counts," *MNRAS* **283**, p. 174, 1996.
11. J.-L. Puget, A. Abergel, J.-P. Bernard, F. Boulanger, W. B. Burton, F.-X. Désert, and D. Hartmann, "Tentative detection of a cosmic far-infrared background with COBE," *A&A* **308**, p. L5, 1996.
12. P. Madau, "The evolution of luminous matter in the universe," in *The Hubble Deep Field*, M. Livio, S. M. Fall, and P. Madau, eds., STScI Symposium Series, 1998. *astro-ph/9709147*.

13. I. Smail, R. J. Ivison, and A. W. Blain, "A deep sub-millimeter survey of lensing clusters: A new window on galaxy formation and evolution," *ApJ* **490**, p. L5, 1997. [astro-ph/9708135](#).
14. D. H. Hughes, S. Serjeant, J. Dunlop, M. Rowan-Robinson, A. Blain, R. G. Mann, R. Ivison, J. Peacock, A. Efstathiou, W. Gear, S. Oliver, A. Lawrence, M. Longair, P. Goldschmidt, and T. Jenness, "Unveiling dust-enshrouded star formation in the early universe: a sub-mm survey of the Hubble Deep Field," *Nature* **393**, p. 241, 1998. [astro-ph/9806297](#).
15. I. Smail, R. Ivison, A. Blain, and J.-P. Kneib, "Deep sub-mm surveys with SCUBA," in *After the Dark Ages: When galaxies were young (the Universe at $2 < z < 5$)*, Maryland Astrophysics Conference, 1999. [astro-ph/9810281](#).
16. E. A. Richards, "Radio identification of sub-mm sources in the Hubble Deep Field," *ApJ (Letters)* **513**, p. L9, 1999. [astro-ph/9811098](#).
17. B. Guiderdoni, E. Hivon, F. R. Bouchet, and B. Maffei, "Semi-analytic modelling of galaxy evolution in the IR/sub-mm range," *MNRAS* **295**, p. 877, 1998. [astro-ph/9710340](#).
18. D. Hughes and J. Dunlop, "Using new submillimetre surveys to identify the evolutionary status of high- z galaxies," in *Observational Cosmology with New Radio Surveys*, 1997. Preprint available on WWW at <http://www.roe.ac.uk/research/dhh2.ps.gz>.
19. P. F. Goldsmith, *Quasioptical Systems: Gaussian Beam Quasioptical Propagation and Applications*, IEEE Press, 1998.
20. D. J. Schroeder, *Astronomical Optics*, Academic Press, 1987.
21. A. A. Stark, J. E. Carlstrom, F. P. Israel, K. M. Menten, J. B. Peterson, T. G. Phillips, G. Sironi, and C. K. Walker, "Plans for a 10-m submillimeter-wave telescope at the South Pole," in *Advanced Technology MMW, Radio and Terahertz Telescopes*, vol. 3357, pp. 495–506, Proceedings of SPIE, 1998. [astro-ph/9802326](#).
22. C. Dragone, "A first-order treatment of aberrations in Cassegrainian and Gregorian antennas," *IEEE Trans. Antennas and Propagation* **AP-30**, p. 331, 1982.
23. "The Green Bank Telescope." <http://info.gb.nrao.edu>.